arXiv:1610.09143v1 [quant-ph] 28 Oct 2016

Measuring the deviation from the superposition principle in interference experiments

G.Rengaraj [1], U.Prathwiraj [1], Surya Narayan Sahoo [1],
R.Somashekhar[1], and Urbasi Sinha [1]

[1]Raman Research Institute, Sadashivanagar, Bangalore, India.

*To whom correspondence should be addressed; E-mail: usinha@rri.res.in.

The superposition principle forms the heart of all modern applications and properties of Quantum Mechanics including Quantum Computing and Quantum Entanglement. However, its usual application to slit based interference experiments has caveat in both Optics and Quantum Mechanics where it is often incorrectly assumed that the boundary condition represented by slits opened individually is same as them being opened together. Error entailed by this assumption is quantified by a parameter which has been calculated by recent theoretical works to be non-zero under correct boundary conditions. No experiment till date has reported a non-zero value for this quantity κ yet. Here we report the first measurement of a non-zero κ of the order 10^{-2} in the microwave domain using antennas as sources and detectors of the electromagnetic waves. With remarkable agreement between experiment and theory, we convincingly demonstrate the deviation from the usual application of the superposition principle. We also show that our results can have potential applications in formulating better error models in observational radio astronomy

data in studies of the epoch of reionization of the early universe where similar naive assumptions are sometimes made about the application of the superposition principle.

Young's double slit experiment plays a pivotal role in Physics especially Optics and Quantum Physics. In Classical Optics, it demonstrates the wave nature of light. In the quantum mechanical domain when performed using single particles, it is a classic demonstration of the wave-particle duality of light and matter. Nobel laureate Richard Feynman famously said that it contains within it all the mysteries of Quantum Mechanics. Having said that, how well do we understand the various facets of the double slit experiment?

One of the assumptions that is commonly made in expositions of the double slit experiment is about superposition of the solutions to the wave equation with slits opened individually being the same as the solution with both slits opened at the same time. For instance, in a double slit set-up, if the solution to the wave equation with slit A open is given by amplitude ϕ_A and the solution with slit B open is given by amplitude ϕ_B, then the solution when both slits are simultaneously open is commonly taken to be $\phi_A + \phi_B$ (*1–5*) . This is done both in the classical domain for instance superposing solutions to the Maxwell equations as well as in the quantum domain for instance superposing solutions to the Schrodinger equation. The fact is that this naive application of the superposition Principle is not strictly true in both classical and quantum domains as solutions can only be superposed when they satisfy the same boundary conditions. This was quantified by (*1*) where the authors theoretically quantified the deviation in terms of the normalized version of the Sorkin parameter κ (*7*), which turns out to be non-zero when the boundary conditions are correctly taken into account. In their work, the authors used the Feynman Path Integral formalism to quantify the effects. In the formalism, classical refers to paths which extremize the action whereas non-classical refers to the sub-leading paths which do not extremize the action. Representative paths are shown in the inset of Figure 1. When only classi-

cal paths are accounted for, κ is manifestly zero. Taking into account non-classical paths which actually represent the deviation from the superposition principle makes κ a non-zero quantity. It was found that simulations in (*1*) were equally applicable to both the quantum and classical domain. This was followed by an analytic version of the work (*2*). In (*7*), Finite Difference Time Domain simulations of κ were carried out which showed that the boundary conditions play a crucial role in the classical electromagnetic domain.

The importance of boundary conditions was first pointed out by Yabuki (*10*) in his theory work involving path integrals and double slits. However, although there has been a lot of theoretical interest in this problem over the last few years, all experiments to measure this quantity so far (*3–5, 11–13*) have been unable to report a non zero value for κ due to the error contribution being much larger than the expected non-zeroness of κ. In this paper, we report measurement of a non-zero Sorkin parameter for the first time which is much above the error bound. We have performed a precision experiment on an open field in the centimetre wave domain using pyramidal horn antennas as sources and detectors of electromagnetic waves and specially manufactured composite materials as microwave absorbers to provide us with the slots. The measured graphs of κ as a function of detector position have good agreement with theoretically simulated plots using the Method of Moments (which is a 3D simulation technique in which exact horn detector and slot material parameters can also be simulated). These results indicate the importance of taking proper boundary conditions into consideration while applying the superposition principle in slit/slot based interference experiments. This is a generic result and does not need a quantum mechanical explanation per se. They also exemplify a situation in which *not* just the classically dominant paths in the Path Integral formalism has been used to explain experimental observations. In some sense, they bring forth the experimental reality of the winding paths in Path Integrals.

In this paper (*18, 19*), we report results of a triple slot experiment. As the dimensions are macroscopic (centimetre scale), for a commensurate slit based experiment, in order to consider a suitable outer box for simulations, we would need to etch the slits in an absorbing layer which needs to be several metres long. This is both practically and economically prohibitive. On the other hand, having absorbing slots surrounded by free space it is much simpler to mimic infinitely large boundaries.

The definition of κ in case of the triple slot experiment becomes:

$$\kappa = \frac{p_{BG} - (p_{ABC} - p_{AB} - p_{BC} - p_{CA} + p_A + p_B + p_C)}{Max(p_{BG})}, \tag{1}$$

where p_{BG} is the magnitude of the Poynting vector at a certain detector position due to the horn source (in experiment, it is the measured power value) and $Max(p_{BG})$ is the maximum value of the same. p_x stands for magnitude of the Poynting vector at a certain detector position due to the presence of slot combination x where $x = A, B, C, AB, BC, AC, ABC$. Further details on the above definition are included in (*20*).

Figure 1 shows the details of the experimental set-up. We have a pyramidal horn antenna acting as a source of electromagnetic waves at 5 cm wavelength. These waves are incident on slots which are 10 cm wide having an inter-slot distance of 13 cm (centre to centre). The slots are composite structures which consist of two layers of specially manufactured materials which act as near perfect absorbers of microwave frequency (Eccosorb SF6.0) sandwiched with an aluminium layer in between to enable even more perfect absorption especially of back reflected beams which may make their way back to the source antenna from the detector. We have done some rigorous analysis of such back reflection and concluded that they do not affect our experiments. This is included in (*20*). The detector antenna is also a horn antenna similar to the source but housed on a moving rail to enable collection of data as a function of detector position. We use a high frequency power probe to record power values for the different combinations of

slots required for measuring κ as a function of detector position. The measurement involves eight separate experiments which measure the individual contributions to equation 1. A ninth measurement involves measuring with source off and detector on to confirm that the antenna does not pick up any comparable signal from unknown emitters in the environment. We found that this was several orders of magnitude lower than the measured values with the source on and that our stray signal level is very low. We also have a corn field behind our detector antenna which surprisingly mimics a perfectly matched layer. In the Methods section in (*20*), we have included technical details on how we aimed at achieving perfect alignment which plays a crucial role in a precision experiment like this one.

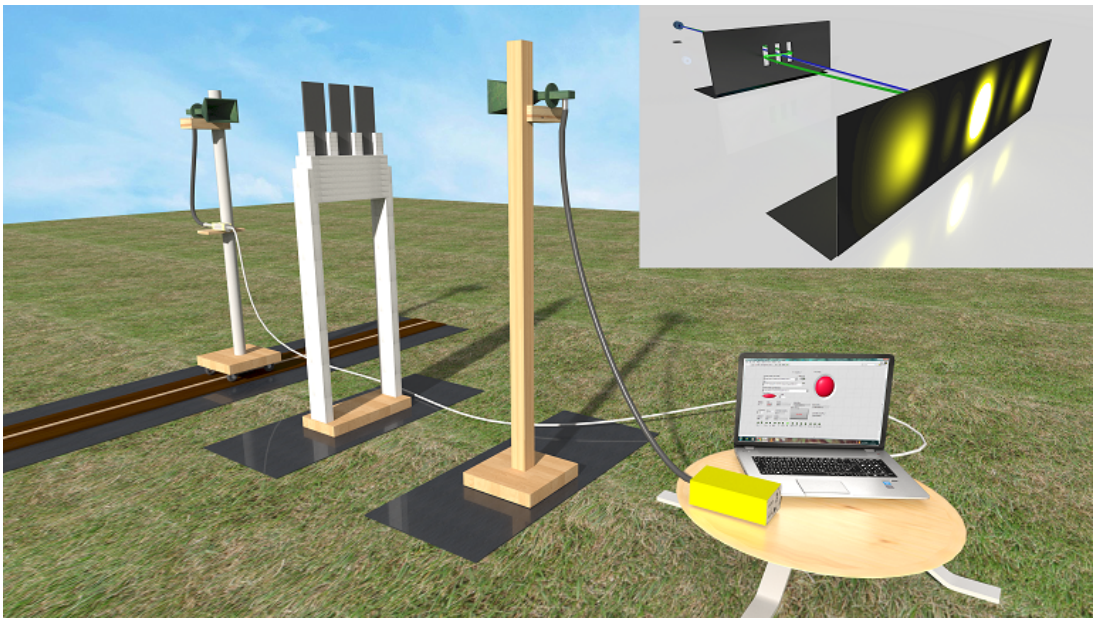

Figure 1: A schematic of the experimental set up. The green antennas on either side are pyramidal horn antennas which act as the source and detector of electromagnetic waves respectively. The detector antenna is placed on a moving rail to enable measuring of diffraction patterns. The three slots are placed between the source and the detector. The inset shows a triple slit schematic where the blue line is a representative classical path and the green line a representative non classical path in path integral formalism.

Figure 2 shows a representative plot of κ as a function of detector position at a source

detector separation of 2.5 metres (1.25 metres between source and slots plane and same distance between slot plane and detector plane). The detector movement is controlled using a 10 RPM DC motor. At each detector position, all eight contributions to equation 1 are measured by placing and removing slots as required before the detector is moved to the next position. This way, we ensure that the κ value at a certain detector position is measured on a short time scale and fluctuations due to the environment do not affect the individual contributions in such a way that it can affect the value of κ measured. We have ensured that our measurement time scale is sufficient by actually measuring an antenna radiation pattern as a background measurement before measuring the pattern due to a particular slot combination. These background patterns overlap during the κ measurement time indicating that our noise fluctuation time scale is much longer than the measurement time. The background corresponding to a certain slot combination is taken to be the average of the background value measured before the combination and after. The formula for κ measured experimentally is modified as follows.

$$\kappa = (P_{ABC} - P_{AB} - P_{BC} - P_{CA} + P_A + P_B + P_C) \times \gamma, \tag{2}$$

where $P_\alpha = \frac{p_{BG\alpha} - p_\alpha}{p_{BG\alpha}}$, $\alpha = A, B, C, ...ABC$ slots being present and $p_{BG\alpha}$ refers to the background corresponding to each combination. $\gamma = \frac{p_{BG(at\ x=x_D)}}{p_{BG(x=0)}}$, x_D being a certain detector position where $x = 0$ is the central position. As can be seen, at the central position, $\gamma = 1$ and the equations 1 and 2 become equivalent. By defining individual background contributions to the different terms in equation 1, we can take care of varying source power, if any, between combinations. The background value is measured using a reference detector and also by averaging between background values measured before and after each combination which turn out to be equivalent in our case.

For each combination, 3000 data points are collected, the average of which contributes the

measured power value. Thus each κ value has 3000 measured values for each combination. The number 3000 was arrived at after sampling for both lower and higher number of data points. 10 measurements of κ were done at each detector position and the median value has been chosen as the representative value. The errors for each value have been represented by box plots (*14*). Further details on choice of measurement statistics as well as error analysis are given in (*20*). We have also randomised the order in which slot combinations are measured and ensured that κ remains constant.

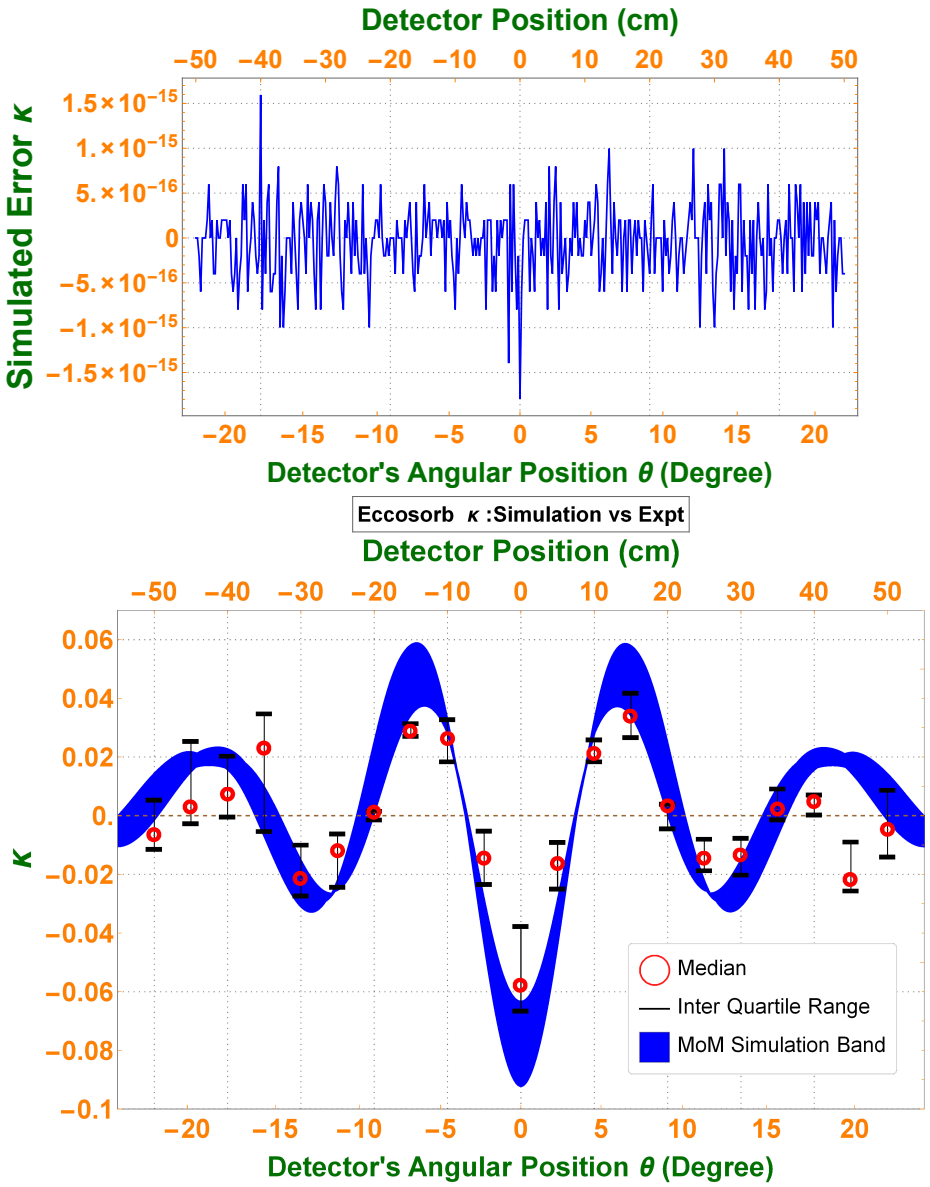

Figure 2: The plot on top is a simulation result which is a plot of κ as a function of detector's angular position (which is the angle subtended at the detector plane by the centre of the slot plane) when the superposition principle is incorrectly applied. We have obtained this by taking into account only classical paths in the path integral formalism whereby κ is manifestly zero. The plot below is a representative experimentally measured κ as a function of detector's angular position. The red markers represent the median κ at each position. The black lines denote the interquartile range in the box plot. We have removed outliers from the plot. The blue band represents the theory band obtained from Method of Moments based simulation. In order to create the theory band, we simulated κ for the experimental parameters taking into account uncertainties in various experimental parameters. The major contributions to the band came from antenna probe wire height, distance from backplate, interslot distance as well as the material refractive index based uncertainties.

Figure 3 shows measured κ as a function of detector position for two different source-detector distances. This was done to ensure that the match between theory and experiment persists even on changing some changeable parameters in the experiment.

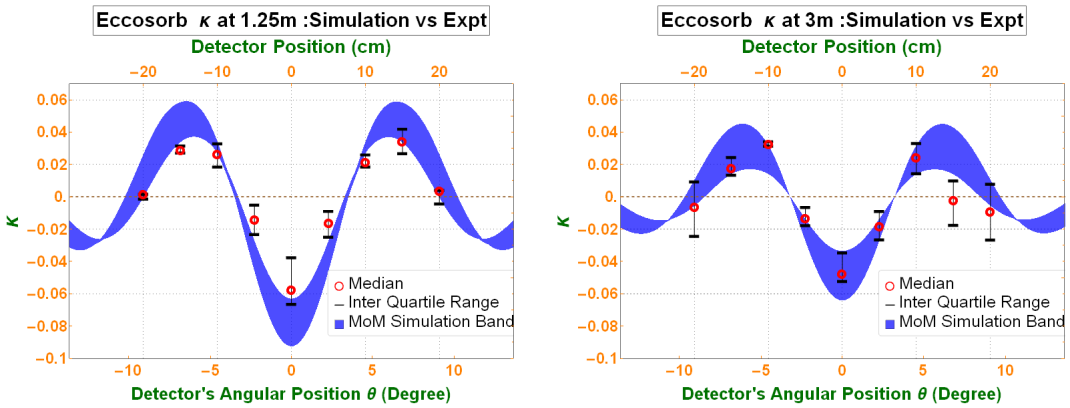

Figure 3: The graph on the left is for source-slot plane distance of 1.25 m. The graph on the right is for source-slot plane distance of 3 m. The distance between slot plane and detector plane is kept 1.25 m in both cases. As can be seen experiment and theory match very well in both cases. Theory predicts a drop in the κ values with increasing source-slot distance which is corroborated by experiment. As distance increases, the noise remains similar but signal drops making signal to noise go down which results in generally bigger error bars at larger distance.

We have performed some other simulation based tests, details of which are included in (*20*). We have simulated the effect on κ from changing detector size inspired by observations in (*3*) and found that detector size does not play a significant role in our measurements. We have done simulations using path integral formalism and Finite Difference Time Domain simulations and compared the same. We have also added absorbers perpendicular to the slots (in between the slots) to in principle "kill" the effects due to non classical paths and seen the reduction in κ with increasing size of such absorbers which we call baffles.

One of the main errors which can lead to observation of a non-zero κ will be the non-

linearity if any of the detector. If a detector behaves non-linearly with increase in incident power, then the quantity in equation 1 will automatically be a non-zero just from such errors. We have done detailed analysis of detector non-linearity (details in (*20*)) and found that our measured κ cannot be explained by any such non-linearity which happens to be much below the measured κ. In our analysis, we have derived a non-linear function for the detector using both spline interpolation method as well as polynomial fit and derived the resultant κ from this function. We have found the κ value so derived to be much lower than the measured κ thus indicating that the non linearity effects do not play a major role in our experiment.

The experimental result reported in this manuscript has several implications in optics as well as related areas of research like Radio Astronomy. In the latter, the community is divided in the sense that while some work in available literature seems to take into account boundary condition effects (*21, 22*), there are others which seem to ignore them (*6, 23*). We have explored this application in further detail and found that by taking relevant parameters from such experiments (*6*), we get κ to be of the order of 10^{-2} which is definitely not ignorable any more considering that here we are reporting an experiment where we have successfully measured the quantity much above the error bound. There are some applications in this field where the naive application of the superposition principle is routinely used, for instance in calculation of array factor (*25*) as well as in estimation of effects of badly behaving antennas in an array configuration. We find that for very large arrays, such approximations may hold upto a point; however, the gain calculated using correct boundary conditions (MOM simulations) gives much better match that array factor at higher angles. The validity of the approximations is inversely proportional to the array size and is also dependent on whether the absolute power value is of concern (in which case boundary conditions play a big role as opposed to normalization with bright sources in the sky). In any event, our current experimental results and calculations using radio astronomy parameters tells us that these boundary conditions will play a crucial role in future experiments

on precision Cosmology where errors from other sources would have been suitably minimized. We have included further details on our analysis as well as the κ graph obtained in (*20*).

Being a first non zero detection of the normalized Sorkin parameter, our experiment helps vindicate the recent claims of different theory papers that the superposition principle when applied to slit based interference experiments needs a correction term originating from the difference in boundary conditions presented between multiple slits opened all at once compared with a summation of the effects from the slits being opened one at a time (*1, 2, 7, 10*). This is a fundamentally important experimental result and is expected to play a major role in the quest for genuine post quantum higher order interference. Higher order interference was initially discussed by Sorkin (*7*) in the framework of Quantum Measure Theory. Recently, a lot of theoretical thrust has gone towards developing what are called generalized probabilistic theories (*26*) **which actually require as a postulate that higher order interference be zero**. Our work which puts a non-zero bound on higher order interference from boundary condition arguments then naturally raises the following question: What will change now that the Sorkin parameter has been proven to be non zero within the realms of quantum physics and classical electromagnetism? Does this non-zeroness affect such post quantum theories (*27, 30*) and if so, how? Finally, a question of much practical significance arises. Since genuine higher order interference is being investigated as a possible resource in computation (*28, 29*), how will the experimental verification that higher order interference turns out to be non-zero affect such research directions?

References and Notes

1. Feynman, R. P. Leighton, R. & Sands, M. *The Feynman Lectures on Physics Vol. 3* (Addison - Wesley, Reading Mass, 1963).

2. Cohen-Tannoudji, C. Diu, B. & Laloe, F. *Quantum Mechanics I*, (Wiley - VCH, 2nd edition, 2005)

3. Shankar, R. *Principles of Quantum Mechanics*, (Springer, 2nd edition, 1994).

4. Born, M. and Wolf, E. *Principles of Optics* (Cambridge University Press, Seventh expanded edition, 1999).

5. Feynman, R. P. & Hibbs, A. R. *Quantum Mechanics and Path Integrals* (McGraw-Hill, New York, 3rd. ed. 1965).

6. R.Sawant, J.Samuel, A.Sinha, S.Sinha and U.Sinha. *Phys. Rev. Lett.* **113**, 120406 (2014).

7. Sorkin, R. D. Quantum mechanics as quantum measure theory. *Mod. Phys. Lett. A*. **9**, 3119 (1994).

8. A.Sinha, Aravind H.Vijay and U.Sinha. *Scientific Reports* **5**, 10304 (2015).

9. Raedt, H.D. Michielsen, K. Hess, K. Analysis of multipath interference in three-slit experiments. *Phys. Rev. A*. **85**, 012101 (2012).

10. Yabuki, H. Feynman path integrals in the young double-slit experiment. *Int. J. Theor. Ph.* **25**, No.2, 159-174 (1986).

11. U. Sinha, C. Couteau, T. Jennewein, R. Laflamme, R. Weihs, G. Ruling out multi-order interference in quantum mechanics. *Science* **329**, 418-421 (2010).

12. Söllner, I. *et al*. Testing born's rule in quantum mechanics for three mutually exclusive events. *Found Phys*. **42**, 742-751 (2012).

13. Park, D. K. Moussa, O. Laflamme, R. Three path interference using nuclear magnetic resonance: a test of the consistency of Born's rule. *New J. Phys*. **14**, 113025 (2012).

14. Chambers, J.; Cleveland, W.; Kleiner, B.; and Tukey, P. Graphical Methods for Data Analysis. Belmont, CA: Wadsworth, 1983

15. E.Gagnon, C.D.Brown, A.L.Lytle, Effects of detector size and position on a test of Born's rule using a three-slit experiment. *Phys. Rev. A***90**, 013832 (2014).

16. T.Kauten, B.Pressl, T.Kauffmann, G.Weihs, Measurement and modelling of the nonlinearity of photovoltaic and Geiger-mode photodiodes. *Rev. Sci. Instr.* **85**, 063102 (2014).

17. T.Kauten, R.Keil, T.Kaufmann, B.Pressl, C.Brukner, G.Weihs, Obtaining tight bounds on higher-order interferences with a 5-path interferometer. arXiv :1508.03253v3

18. Tallk on this experiment by Urbasi Sinha `https://www.youtube.com/watch?v=8bb_HZkEBfg`

19. Talk on this experiment by Urbasi Sinha `http://pirsa.org/displayFlash.php?id=16080023`

20. See Supporting online material

21. D. B. Davidson, R. Lehmensiek, D. I. L. de Villiers, A. Young, Current capabilities for the full-wave electromagnetic modelling of dishes for SKA. *International Conference on Electromagnetics in Advanced Applications (ICEAA)*, 1368-1371 (2013).

22. A. R. Weily, K. P. Esselle, T. S. Bird, B. C. Sanders, Linear array of Woodpile EBG Sectoral Horn Antennas. *IEEE Transactions on Antennas and Propagation*.**54**, 2263-2274 (2006)

23. S. W. Henderson et al, Advanced ACTPol Cryogenic Detector Arrays and Readout. arXiv:1510.02809v1(2015).

24. Saurabh Singh et al, On the detection of global 21cm signal from reionization using interferometers. *The Astrophysical Journal* **815** No.2, 2015

25. Randy L. Haupt, Antenna Arrays: A computational approach. DOI: 10.1002/9780470937464

26. H.Barnum, M.P.Muller, C.Ududec, Higher order interference and single system postulates characterizing quantum theory, *New Journal of Physics*, **16**, 2014.

27. C.M. Lee and John Selby, Higher order interference in extension of quantum theory, arXiv: 1510.03860

28. C.M.Lee and John Selby, Deriving Grover's lower bound from simple physical principles, *New Journal of Physics*, **18**, 2016.

29. C.M.Lee and John Selby, Generalized phase kick-back: a computational advantage for higher order interference?, *New Journal of Physics*, **18**, 033023, 2016.

30. Lorenzo M. Procopio et al, Experimental test of hyper-complex quantum theories, arXiv:1602.01624v2

31. GR and PU contributed equally to the work; GR, PU and SNS performed the experiment; SS helped in instrumentation and field based experience; US conceived of and supervised the experiment; GR, PU, SNS and US contributed to modelling and analysis; US wrote the manuscript. We thank M. Arndt, K.B.Raghavendra Rao, A. Raghunathan, Barry Sanders, R. Subrahmanyan, N. Udayashankar and G.Weihs for useful discussions. We thank A. Sinha and D. Home for reading through the draft and helpful comments and discussions and A. Sinha also for theoretical insights. We thank Anjali P.S, Shreya Ray and Ashutosh Singh for their assistance in the preliminary stages of the project. We thank the staff members

at the Gauribidanur Observatory for use of their facilities for the measurements, as well as mechanical workshop and carpentry section of RRI for their patience in building various versions of our equipment.

Supporting online material for Measuring the deviation from the superposition principle in interference experiments

G.Rengaraj [1], U.Prathwiraj [1], Surya Narayan Sahoo [1],
R.Somashekhar[1], and Urbasi Sinha [1,2]
[1]*Raman Research Institute, Sadashivanagar, Bangalore, India.*
[3] *Institute for Quantum Computing, 200 University Avenue West , Waterloo, Ontario, Canada.*
[*]*To whom correspondence should be addressed; E-mail: usinha@rri.res.in.*

Modification to the definiton of the Sorkin parameter in the slot based interference experiments

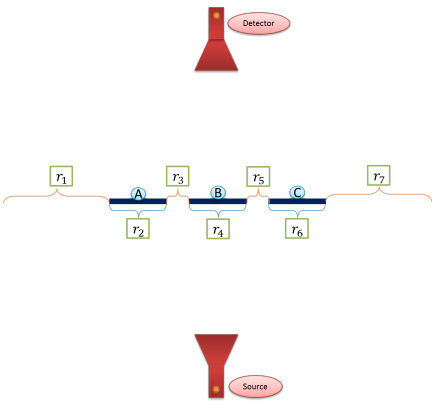

Figure S1: The division of the slot plane into seven regions to explain the modification to the definition of the Sorkin pamater in slot based interference experiments

As seen in Figure S1, in case of a triple slot configuration, the slot plane can be divided into 7 regions. Let us denote the electric field emanating from region"x" as $\vec{E_x}$ and magnetic field as $\vec{H_x}$. Then naive application of the superposition principle gives us the following:

- $\vec{S}_{BG} \propto (\vec{E}_1 + \vec{E}_2 + \vec{E}_3 + \vec{E}_4 + \vec{E}_5 + \vec{E}_6 + \vec{E}_7) \times (\vec{H}_1 + \vec{H}_2 + \vec{H}_3 + \vec{H}_4 + \vec{H}_5 + \vec{H}_6 + \vec{H}_7)$
- $\vec{S}_A \propto (\vec{E}_1 + \vec{E}_3 + \vec{E}_4 + \vec{E}_5 + \vec{E}_6 + \vec{E}_7) \times (\vec{H}_1 + \vec{H}_3 + \vec{H}_4 + \vec{H}_5 + \vec{H}_6 + \vec{H}_7)$
- $\vec{S}_B \propto (\vec{E}_1 + \vec{E}_2 + \vec{E}_3 + \vec{E}_5 + \vec{E}_6 + \vec{E}_7) \times (\vec{H}_1 + \vec{H}_2 + \vec{H}_3 + \vec{H}_5 + \vec{H}_6 + \vec{H}_7)$
- $\vec{S}_C \propto (\vec{E}_1 + \vec{E}_2 + \vec{E}_3 + \vec{E}_4 + \vec{E}_5 + \vec{E}_7) \times (\vec{H}_1 + \vec{H}_2 + \vec{H}_3 + \vec{H}_4 + \vec{H}_5 + \vec{H}_7)$
- $\vec{S}_{AB} \propto (\vec{E}_1 + \vec{E}_3 + \vec{E}_5 + \vec{E}_6 + \vec{E}_7) \times (\vec{H}_1 + \vec{H}_3 + \vec{H}_5 + \vec{H}_6 + \vec{H}_7)$
- $\vec{S}_{BC} \propto (\vec{E}_1 + \vec{E}_2 + \vec{E}_3 + \vec{E}_5 + \vec{E}_7) \times (\vec{H}_1 + \vec{H}_2 + \vec{H}_3 + \vec{H}_5 + \vec{H}_7)$
- $\vec{S}_{CA} \propto (\vec{E}_1 + \vec{E}_3 + \vec{E}_4 + \vec{E}_5 + \vec{E}_7) \times (\vec{H}_1 + \vec{H}_3 + \vec{H}_4 + \vec{H}_5 + \vec{H}_7)$
- $\vec{S}_{ABC} \propto (\vec{E}_1 + \vec{E}_3 + \vec{E}_5 + \vec{E}_7) \times (\vec{H}_1 + \vec{H}_3 + \vec{H}_5 + \vec{H}_7)$

We see that if we compute the numerator of κ defined for slits

$$num(\kappa) = p_A + p_B + p_C - p_{AB} - p_{BC} - p_{CA} + p_{ABC} = pBG \tag{3}$$

Here $\vec{S_\alpha}$ denotes the Poynting vector corresponding to a slot combination α and p_α denotes the real part of the Poynting vector which is the same as the magnitude of the Poynting vector in the radiative zone of the antenna. Thus, we can define the new numerator to be

$$p_{BG} - num(\kappa_{slits}) \tag{4}$$

which is zero when we apply the superposition principle incorrectly. Although the scalar field calculation is shown here, we have verified that

Thus, we define kappa for slots as

$$\kappa_{SLOT} = \frac{p_{BG} - (p_A + p_B + p_C - p_{AB} - p_{BC} - p_{CA} + p_{ABC})}{\max(p_{BG})} \tag{5}$$

In our manuscript, κ_{SLOT} will be denoted by κ.

Effect of back reflection from antenna/slots on measured values of κ

When one has metal structures facing each other and one is a source while the other is a receiver, there is a finite possibility that the metal from the receiver will reflect some radiation back to the source as a result of which the radiation from the source will have an additional effect added to it. In case of the current experiment which falls in the domain of precision experiments, it becomes very important to establish that such variations if any in the source radiation does not lead to a"false" non-zero κ. In the current experiment, there are three different ways in which such effects can be expected to play a role and we have systematically investigated all such effects and eliminated them as major contributors to our measured κ.

The first investigation involved varying the source-receiver distance and measuring the receiver power as a function of detector position at increasing distances. While we found that there is some fluctuation and variation in the measured power for short distances between the source and

receiver as expected, as the distance increased, the receiver power settled down to a constant value. This happens at about 50 cm distance between the flares of the apertures of the two horn antennas. Our experiment has been carried out at a distance of 2 metres between the two horn flares and thus we are way beyond any distance where such effects matter. We also checked the same effects by removing the horn structure and just retaining the probe wires and found that the fluctuations again drop beyond a 50 cm distance between the horn flares. The presence of horn causes oscillations typical of a cavity structure which does not occur in the absence of horn. The presence of the horn of course is very useful in increasing the gain by orders of magnitude. All oscillations and fluctuations occur at much closer horn to horn distance than in our experiment. We calculated the maximum effect that any such reflection can have on κ and found that the effects are more than one order of magnitude lower than the measured κ. One could argue at this point that since increasing the distance between source and receiver gets rid of unwanted effects, why not make it even larger? We simulated the effects at a larger distance of 8 metres and while the simulated effects were lowered further, so did the actual power. The signal to noise thus did not change significantly. On the other hand, in terms of measured power, in order to achieve more than three orders of precision, the minimum incident power should be in the micro-watt regime which is difficult to achieve at 8 metres distance given our maximum output from the signal generator. By choosing the distance to be 2 m instead of 8 m, the detected power roughly increases by a factor of 16 along with a larger predicted value of κ. This sealed our choice for 2 m distance between the horn flares which is 2.5 m distance between the probe wires for our experiment.

The second investigation involved moving the horn detector in the transverse direction at the desired 2 m distance to ensure that any resultant interference effects do not contribute unwanted effects. We found that the maximum effect from such traverse is also lower order in magnitude that our expected κ. We can thus conclude that most of our non-zero κ values are above the

maximum error threshold from such horn structure reflections.

The third investigation requires us to introduce a concept which we would like to call "errror κ". What we are verifying in this experiment is the deviation from the naive application of the superposition principle. While the naive application gives us an expected zero value for κ, the correct application brings forth the non-zeroness. One way in which we have investigated different genres of errors in our experiment is by defining what we call "error κ". Following references (*1*) and (*2*), we define κ only in the presence of"classical" paths or in other words when the Superposition principle is naively applied. This is expected to be zero in ideal theory. However, in case of real experimental/simulation scenarios which involve non-ideal conditions, this quantity can be a non-zero. One has to appreciate that this non-zero is simply due to different sources of error as the case may be and has nothing to do with the correction to the application of the Superposition principle which is a"real" non-zero as opposed to an error bound. We call such an error bound"error κ." This quantity derived simply from the terms involving classical paths comes in very handy as it tells us whether some source of error has a competing effect with the actual non-zero value. Thus if error κ is lower order in magnitude than actual κ, we need not worry about a particular error playing a dominant role in explaining the non-zeroness of κ.

When we place slots directly in front of the horn source, the slots may reflect some fields back to the source which could also in principle cause the emitted source profile to change. As our experiment involves changing the slot configuration seven times, these back reflections can lead to changing source profiles for each such case which in turn can lead to a non-zero κ simply due to the changing source term. We used the Method of Moments method to calculate the complex current in the probe wire for various slot combinations. Then we used these complex currents to appropriately scale the source wave function for each combination. As the current in the probe wire will change for different slot combinations due to the effect of back reflections,

this will lead to different source powers for different combinations. These can then be used to estimate error κ. Figure S2 shows the error κ calculated for our heterostructure material using a vertically oriented wire as a source.

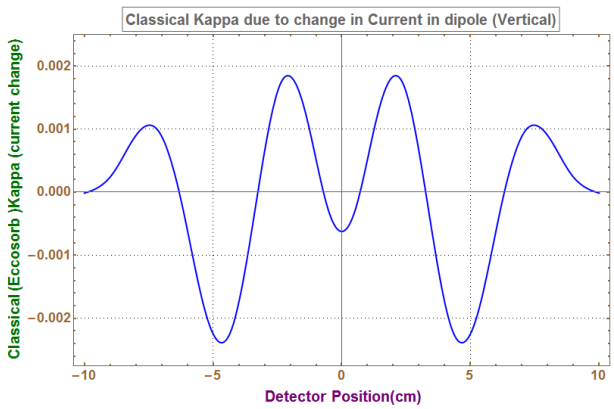

Figure S2: κ due to current change in dipole for heterostructure slots

We see that κ, if at all is due to change in source, is 0.0025 or less (almost 50 times less than the actual κ).

For metals, we take the horn source and carry current in the horn wire probe. We found the kappa computed from this method is five times less than simulated kappa(about 0.3).

The final investigation involved simulating error effects in absence of horn structure as well as metal probe. This will decide whether the simulated effects are due to reflections from the metal in the horn structure itself or mutual coupling between the probe wires. First, for the background combination, the complex electric and magnetic fields at the horn source aperture were calculated. The above fields are then imposed in the simulation i.e. they are assumed to be there without any probe wire as well as horn metal structure. The same source is imposed for every combination thus guaranteeing an invariant source. If there is a difference in the κ graph between the case where the source is thus imposed to be invariant and when the actual horn structure with the probe wire acts as a source, then this can be attributed to spurious effects

due to back reflection and mutual coupling etc. Figure S3 shows the κ graph obtained for metal slots and screen detector with source-detector horn flare distance of 2 m. As can be seen, except a slight change at the centre, the two graphs show remarkable agreement thus ruling out back reflections as playing any dominant role in our measured values. One should note that since in the metal slot case, the effect can be ignored, the same will of course hold even for the heterostructure based experiments where the slots have been custom made to be maximally absorbant.

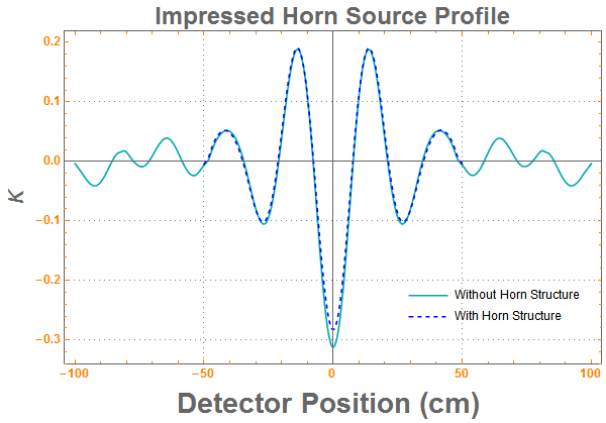

Figure S3: Metal Slots, Screen detector at 100 cm from slot plane. Kappa with the imposed invariant source and the actual horn structure show remarkable agreement.

Methods

Alignment

One of the most crucial steps which enables us to measure a convincing non-zero for κ involves precise alignment of the various components in the experiment. While there is alignment at a basic level, there is also finer alignment using dedicated tools.

- The first condition to be ensured is perfect levelling of the ground. A spirit level is used at various points on the ground to check the ground level and all unevenness is filled with sand. One preliminary levelling is achieved, we place a marble-like stone on the ground

to ensure further smoothness. These stones need to be settled into the ground using water so that once set, they do not sag any further. Figure S4 illustrates ground levelling.

Figure S4: Once the ground has been levelled using sand and spirit level, the portions which house experimental components are further levelled using set stones

- The experimental set-up consists of a rail, a motor for horn antenna detector movement, two horn antennas, slot stand and slots. The source horn antenna is connected to an Anapico signal generator which generates microwaves at 6GHz. The receiver horn antenna is connected to a high frequency power probe from Agilent. The power probe is controlled by using Labview.

- The next alignment involves alignment of transmitter and receiver horn antennas.

- The transmitter horn antenna is fixed while the receiver antenna moves on a rail. For initial alignment, the receiver antenna is placed at the centre of the rail directly in front of the source antenna. It is ensured that the two antenna centres coincide with each other. This is done using a plumb line.

- Once the perpendicular alignment is done, one needs to ensure that the distance between the edge of the rail on either side is the same from the source. This is done using a Laser Distance metre (LDM).

- Next, the slot stand (made of high density thermocol which is separately checked to be a perfect transmitter for the 6GHz microwaves upto the desired accuracy)is placed between the source and receiver. The distance between the source antenna probe wire and the receiver antenna probe wire is 2.50 metres and the slot stand is exactly 1.25 metres from each. The distances are again ensured using LDM.

- Water level is used to ensure that the height of both the source and receiver antennas are 1.75 metres from the ground.

- Figure S5 shows a picture of the set-up.

Figure S5: A real view of the set up post alignment

- Figure S6 shows the distances between various components.

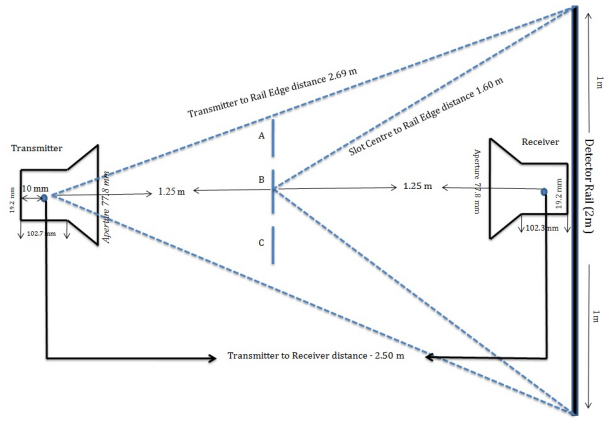

Figure S6: schematic of distance between various components in the experiment

- Figure S7 shows the final set up which is housed in an appropriate tent for protection against wind and rain.

Figure S7: Final experimental set up which is housed in a tent

Ground reflection measurements

One of the considerations that plays a role in experiments which are performed in open field conditions is the possibility of reflection from the ground affecting the source radiation. Other than the back reflections from metal and other structures on the field (which we have discussed

in the section above), we also need to confirm that reflections from the earth's surface do not cause any difference in measured power. One can reduce the effective reflection from the ground by raising antenna height to an extent that these reflections do not play any role. Figure S8 shows a plot of measured power vs height of source and receiver antenna at different source powers (0dBm, 10dBm, 15dBm). As one can see, beyond 145 cm height of the antennas, there is no change in power measured. This implies that beyond this height, there is no change caused due to specular reflection. Our experiment was conducted at source and receiver antenna heights of 175 cm.

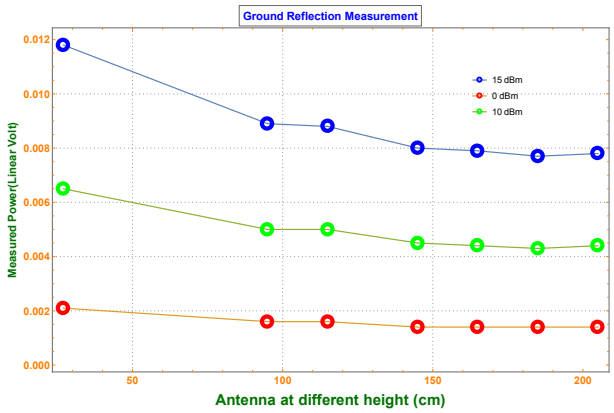

Figure S8: Measured power values as a function of antenna height. The values saturate to the same value beyond 145 cm.

Error Analysis

A precision experiment on an open field may seem like incompatible conditions. Thus, a lot of time and work has gone into ensuring proper representation and accountability of all possible errors. Both random and systematic errors can affect the experiment. A fluctuating source power will add uncertainty to measured κ but the mean κ will not be affected. On the other hand, a systematic drift in the source power will make different slot combinations experience different effective source powers which in turn will cause a shift in the mean κ itself. We have

done several hours of source stability analysis and ensured that the error due to fluctuations of the source is much below the required precision level. Our source also does not suffer from drift within the time required to measure a κ value. This has governed the choice of measurement time for each κ value. There are other errors which are unrelated to the source like possible tilt of slot stand, improper fitting on slot in stand etc. We have ensured as near perfect an alignment as possible and repeated the measurement several times to randomize the error further. There are also issues like humidity, temperature change etc which may affect electrical components by affecting change in resistance and we have ensured that we use the components in optimal conditions. Other than experimental errors, in order to have fair comparison between experiment and theory, we also need to ensure that the theory is not for ideal conditions but in fact takes into account the non idealness and associated uncertainties in different components like length parameters and material parameters. This leads to the generation of the theory band.

The formula used in the experiment is as follows

$$\kappa = P_A + P_B + P_C - P_{AB} - P_{BC} - P_{CA} + P_{ABC} \tag{6}$$

where

$$P_\alpha = \frac{P_{BG_\alpha} - p_\alpha}{P_{BG_\alpha}} \tag{7}$$

Now, we calculate P_{BG_α} by measuring background before and after the slot combination α. Each measurement of background consists of taking 3000 readings (about 45 seconds). To compute the mean $\mu(P_{BG_\alpha})$ we average over the 6000 readings (combining the readings before and after). To compute the $\sigma(P_{BG_\alpha})$ we take the std. deviation of 6000 readings. We do the same thing for p_α, the slot combination. From here, we use 6 to compute mean $\mu(P_\alpha)$ where the RHS of 6 are the mean quantities.

We compute the uncertainty in P_α as follows:

$$\delta P_\alpha = \sqrt{\left(\frac{\partial(\frac{P_{BG_\alpha}-p_\alpha}{P_{BG_\alpha}})}{\partial P_{BG_\alpha}}\delta P_{BG_\alpha}\right)^2 + \left(\frac{\partial(\frac{P_{BG_\alpha}-p_\alpha}{P_{BG_\alpha}})}{\partial P_\alpha}\delta P_\alpha\right)^2} \tag{8}$$

In the above equation, we choose to ignore the higher order terms and further assume that background and slot combination powers are independent (in terms of its variation). In the above equation, the partial derivatives are calculated by first taking the partial derivative and then substituting the means. For the variations, the std deviation is used.

This gives us error in each effective slot combination. Then the mean kappa for a data set is computed using 6 where in RHS all the quantities are mean for each effective slot combination.

The error in κ is simply computed as

$$\sigma_\kappa = \sqrt{\sum(\sigma_{P_\alpha})^2} \tag{9}$$

We have decided to measure 10 κ values at each detector position. If the standard deviation of the mean of a certain number of readings is lower than the average error bars of each data set, then we can say the experiment is reproducible. In our case, 10 data sets satisfied this criterion.

However, the distribution of κ over10 datasets is not normal. Therefore specifying mean and standard deviation does not give the correct impression. Hence, we represent the data in box plot, where we have

- The median of the distribution
- The interquartile range : The range that covers (Q_1) 25% to (Q_3)75% of the data
- Near outliers, Any data point beyond $Q1 - 1.5(Q3 - Q1)$ or $Q3 + 1.5(Q3 - Q1)$ is called a near outlier.
- Far outliers, Any data point beyond $Q1 - 3(Q3 - Q1)$ or $Q3 + 3(Q3 - Q1)$ is called a far outlier.

In our results plot in the main text, we have chosen to ignore the outliers.

Effect on κ due to changing detector size

Following up on (*3*), we have simulated the effect of changing detector size on κ. The detector size is varied as a fraction of the mean experimental aperture size value. It is varied uniformly for both E and H plane. Zero aperture size represents a screen detector. The uncertainty band has been formed by taking into account uncertainties in experimental parameters and the plot in Figure S9 indicates that our measured κ value does not depend significantly on detector aperture size.

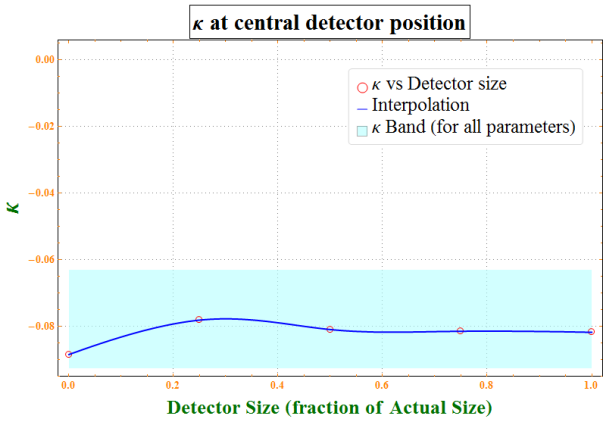

Figure S9: κ at the central detector position as a function of varying detector aperture size

Detector Non linearity analysis

One of the bottlenecks for previous experiments on the measurement of the Sorkin parameter has been the non linearity of the measuring device (*4*). If the detector is non linear, then that can lead to an apparent non-zero κ which is just due to such errors. We have analysed this for our experiment and found that detector non linearity effects, if any, are below the measured κ values and do not explain our results. Figure S10 shows four plots.

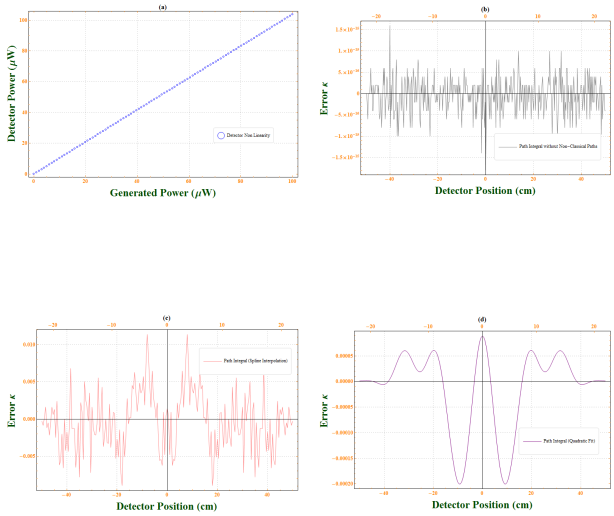

Figure S10: a) measured power values versus input power b) κ generated from classical paths only c) κ generated from spline interpolation method d) κ generated from polynomial fit.

Plot (a) shows measured power values in our Agilent power probe with an Agilent signal generator acting as a source. If the detector is perfectly linear, then the measured value will be exactly the same as the input value. However, no detector can be linear upto arbitrary accuracy. We have used this plot to generate non linear functions from both spline interpolation method as well as polynomial fit. Plot (b) shows the κ that is generated using only classical paths in the path integral formalism. As is expected, κ is identically zero (10^{-16} which is the accuracy of our solver). We have used the power values that lead to this zero value for κ and feeding them to the non linear function generated above, derived the power values that would have been measured. The measured value will vary from the input value due to various non linearity effects. Plot (c) and Plot (d) show the resultant κ as a function of detector position. These values represent what we have defined to be $error\ \kappa$ in an earlier section. As they have generated from taking into account only the contribution from the classical paths in path integral formalism, they should have been zero. However, non linearity effects make them non-zero. Two very

important points should be noted here.

- The non linearity effects captured here reflect the maximum non linearity that can affect our experiment which is of course not representative. Even in this worst case scenario based simulation, the values of κ are many times smaller for the interpolation method and two orders of magnitude lower for the polynomial fit. Thus, they do not in any way explain the results obtained in the experiment.

- Plot (a) captures the non linearity not only due to the power probe but also the source signal generator itself. There is no trusted device that one can assume is perfectly linear and use as a source such that only the measurement device non linearity can be captured. In our experiment, the source is used at a constant power and thus non linearity due to the source does not affect us. The effective non linearity seen in our experiment is thus lower than what we have been able to estimate. The issue of a trusted device also existed in previous work (*5*) as there the attenuator was assumed to be a trusted device.

Implications on precision cosmology

Figure S11 shows the configuration that we have used to calculate κ from parameters used in simulations of signals from the epoch of reionization of the early universe (*6*).

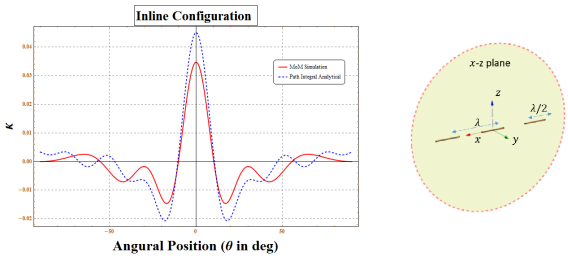

Figure S11: The figure on the left shows κ as a function of detector position. The red line indicates simulation done using Method of Moments. The blue dotted line is the result from the analytical formula based on path integral formalism derived in (*2*). The figure on the right shows the dipole array configuration that was simulated.

We simulate the κ as a function of detector position for an inline array of three dipole antennas. We consider a wire of radius $\lambda/100$ and length $\lambda/2$ with a centre fed port to be an array element (*6*) and measure κ as a function of detector position at $z = 10^3\lambda$ which mimics far field.There are segments along the length of wire due to meshing. When we want to make the wire act as a source, a voltage source is attached to the port which gives $1kV$ voltage across the port. Also the load across the port is kept to be 50Ω when active. When the source is inactive the load across the port is made to be $1M\Omega$. When we want to model the wire as a receiving antenna we don't attach any voltage source across the port. But it does have a load of 50Ω when considered active and a load of $1M\Omega$ when considered inactive. We have confirmed that the reciprocity theorem holds and the resultant graph for the three antennas acting as sources and acting as detectors is the same. (It is more common for antenna arrays to be used as detectors of signals from the early universe but easier for us to simulate the source based configuration). In case of the detector configuration, we take the current at load fo each wire and coherently add them to get the total current at the detector. We then take the absolute square of this to find the power. According to reciprocity, this power has the same value when the the three wires act as source and we measure the power from currents across the load in the detector that is at $z = 10^3\lambda$. For comparison with analytical path integral integral formula (*2*), we need

to move the detector in equal intervals of theta along a circle with a large radius. However, since the power picked up by a metal wire is polarization dependent, we need to orient the wire along x for maximum coupling. Thus there would be an additional $\cos\theta$ factor coming in. To avoid this complication, we compare κ obtained from power obtained from Poynting vector (all components) rather than that of a single polarization. For inline configuration, κ computed from analytical formula and numerical MoM method have similar modulation and magnitude.

κ thus simulated from experimental astrophysical parameters and its convincing match with analytical path integral formula indicates that boundary condition effects are significant even in such experiments. The experimental cosmology community should take note of this result especially in the context of the current experiment which demonstrates that such order of magnitude for the deviation from superposition principle can be convincingly measured. Such effects will be especially significant in precision cosmology experiments where macroscopic error sources would have been eliminated.

Comparison of Path integral result with Finite Difference Time Domain simulations

As earlier theory work on estimating the deviation from the superposition principle was done using path integral formalism (*1, 2*) and Finite Difference Time Domain (FDTD) (*7*), we have also analysed our experiment using these techniques. Figure S12 shows the κ as a function of detector position for our slot experiment parameters using both path integral and FDTD.

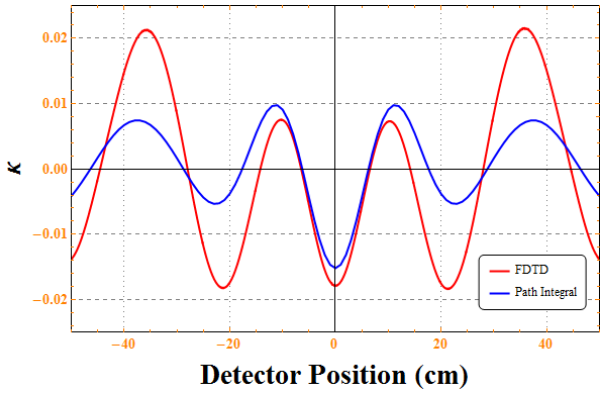

Figure S12: The red line shows κ as a function of detector position obtained using FDTD. The blue line is generated using path integral formalism. The effective slot width in path integral has been taken to be 7 cm as opposed to the actual width of 10 cm. As path integral does not capture material properties, it fails to capture the effect due to waves penetrating the material leading to an effective slot width which is smaller than actual one. This has been discussed in detail in (*2*). FDTD on the other hand has material parameters as input so does not require the concept of effective slot width.

While FDTD and Path Integral show reasonable match in magnitude and modulation, the plot does not match very well with experiments as well as simulations based on Method of Moments. Both FDTD and Path integral have several shortcomings as compared to the full wave Method of Moments (MOM) based simulation. While these are 2D simulations, MOM is 3D. In MOM, one can define the horn source and horn detector while in both these methods, we use point source and point detector. Moreover, being 2D simulations, both FDTD and path integral assume an infinite slot height which is not the case in reality (slot height is 30 cm). Moreover, both path integral and FDTD will have errors as one moves away from the centre. Erros in path integral are due to finite integration domain whereas in FDTD, one has errors due to PML reflections. Over and above these, path integral suffers from some additional limitations. The path integral formalism used in this paper as well in (*1*) and (*2*) is based on scalar field theory whereas FDTD can take into account source polarization. In path integral, material properties need to be accounted for by the concept of "effective width". Also, we use

the thin slot approximation whereas the slot actually has finite thickness.

Inspite of the above limitation, path integral formalism gives the same order of magnitude for κ as well as similar modulation as experiment. Moreover, it serves as a useful aid to distinguish between actual non zeroness of κ and error contributions as the contributions from the non classical paths can be turned off and on at will. It is thus a very handy theoretical tool which is perhaps slightly too ideal to expect perfect match with experiments.

What happens if you use a baffle to reduce the effect due to non classical paths?

Figure S13 shows the conditions for a simulation that we have done in which we have placed blockers (called baffles) perpendicular to the slot plane to in principle kill the effects from the hugging paths in path integral. (*1*) had postulated that the paths which cross the slit plane twice i.e. the hugging paths would have maximum contribution to κ. By placing such perpendicular baffles and simulating κ as a function of increasing baffle size, we find that indeed κ decreases with increase in baffle size. This is a simulation based demonstration that it is indeed this class of non-classical paths which resemble "hugging paths" that contribute maximally to non-zero κ. Figure S14 shows κ at central detector position as a function of increasing baffle size.

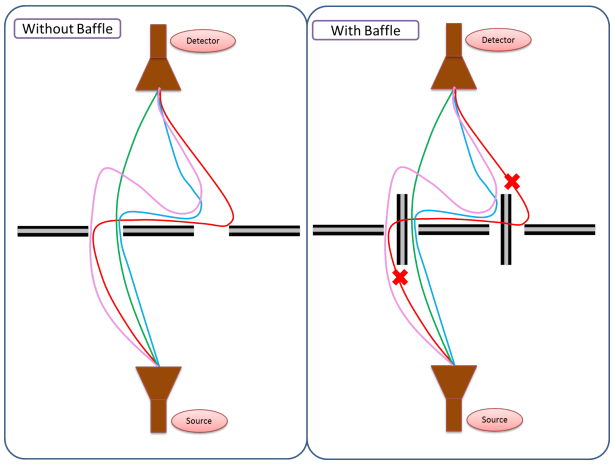

Figure S13: Red lines indicate class of non classical paths that get blocked by baffle, Blue lines indicate class of non classical paths that are still allowed and may contribute to κ, Pink lines indicate class of non classical paths that get suppressed with increase in baffle size, Green lines indicate classical paths

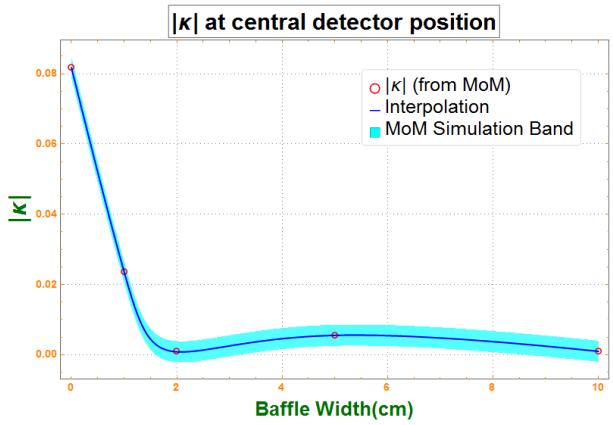

Figure S14: $|\kappa|$ at central detector position as a function of baffle size. Red dots indicate simulated $|\kappa|$ values, blue line is the trend line obtained from interpolation, Shaded blue region is the theory band from Method of Moments simulation

References and Notes

1. R.Sawant, J.Samuel, A.Sinha, S.Sinha and U.Sinha. *Phys. Rev. Lett.* **113**, 120406 (2014).

2. A.Sinha, Aravind H.Vijay and U.Sinha. *Scientific Reports* **5**, 10304 (2015).

3. E.Gagnon, C.D.Brown, A.L.Lytle, Effects of detector size and position on a test of Born's rule using a three-slit experiment. *Phys. Rev. A***90**, 013832 (2014).

4. T.Kauten, R.Keil, T.Kaufmann, B.Pressl, C.Brukner, G.Weihs, Obtaining tight bounds on higher-order interferences with a 5-path interferometer. arXiv :1508.03253v3

5. T.Kauten, B.Pressl, T.Kauffmann, G.Weihs, Measurement and modelling of the nonlinearity of photovoltaic and Geiger-mode photodiodes. *Rev. Sci. Instr.* **85**, 063102 (2014).

6. Saurabh Singh et al, On the detection of global 21cm signal from reionization using interferometers. *The Astrophysical Journal* **815** No.2, 2015.

7. Raedt, H.D. Michielsen, K. Hess, K. Analysis of multipath interference in three-slit experiments. *Phys. Rev. A*. **85**, 012101 (2012).